

Determining the Metallicity of Low-Mass Stars and Brown Dwarfs: Tools for Probing Fundamental Stellar Astrophysics, Tracing Chemical Evolution of the Milky Way and Identifying the Hosts of Extrasolar Planets

Andrew A. West^{1,10}, John J. Bochanski^{2,3}, Brendan P. Bowler⁴, Aaron Dotter⁵, John A. Johnson⁶, Sebastian Lépine⁷, Bárbara Rojas-Ayala⁸, Andreas Schweitzer⁹

¹*Department of Astronomy, Boston University, 725 Commonwealth Avenue, Boston, MA 02215, USA, email: aawest@bu.edu*

²*Astronomy & Astrophysics Dept., Pennsylvania State University, 525 Davey Lab, University Park, PA, 16802, USA, email: jjb29@psu.edu*

³*Kavli Institute for Astrophysics and Space Research, Massachusetts Institute of Technology, Building 37, 77 Massachusetts Avenue, Cambridge, MA 02139, USA*

⁴*Institute for Astronomy, University of Hawai‘i, 2680 Woodlawn Drive, Honolulu, HI 96822, USA, email: bpbowler@ifa.hawaii.edu*

⁵*Space Telescope Science Institute, 3700 San Martin Dr., Baltimore, MD, 21218, USA, email: aaron.dotter@gmail.com*

⁶*Department of Astrophysics, California Institute of Technology, MC 249-17, Pasadena, CA 91125, USA, email: johnjohn@astro.caltech.edu*

⁷*Department of Astrophysics, Division of Physical Sciences, American Museum of Natural History, Central Park West at 79th Street, New York, NY 10024, USA, email: lepine@amnh.org*

⁸*Department of Astronomy, Cornell University, 610 Space Sciences Building, Ithaca, NY 14853, USA, email: babs@astro.cornell.edu*

⁹*Hamburger Sternwarte, University of Hamburg, Gojenbergsweg 112, D-21029, Hamburg, Germany, email: Andreas.Schweitzer@hs.uni-hamburg.de*

¹⁰*Visiting Investigator, Department of Terrestrial Magnetism, Carnegie Institute of Washington, 5241 Broad Branch Road, NW, Washington, DC 20015, USA*

Abstract. We present a brief overview of a splinter session on determining the metallicity of low-mass dwarfs that was organized as part of the Cool Stars 16 conference. We review contemporary spectroscopic and photometric techniques for estimating metallicity in low-mass dwarfs and discuss the importance of measuring accurate metallicities for studies of Galactic and chemical evolution using subdwarfs, creating metallicity benchmarks for brown dwarfs, and searching for extrasolar planets that are orbiting around low-mass dwarfs. In addition, we present the current understanding of the effects of metallicity on stellar evolution and atmosphere models and discuss some

of the limitations that are important to consider when comparing theoretical models to data.

1. Introduction

Low-mass dwarfs are the most numerous stellar constituents of the Milky Way and have main sequence lifetimes that exceed the current age of the Universe (at least for those that are not brown dwarfs). They therefore form an important laboratory for probing the structure and evolution of the Milky Way's disks. Because of their ubiquity, cool dwarfs may represent the largest population of stars with orbiting planets, especially low-mass planets in their respective habitable zones, which are considerably closer for cool dwarf systems. In addition, the diminutive sizes of these stars makes the detection of transiting planets easier than for higher mass stars (for any given planetary radius). Previous results have demonstrated that planets are more likely to be found orbiting metal-rich stars (e.g. Fischer & Valenti 2005). There were preliminary indications that the M dwarfs with known planets had sub-solar metallicities (Bonfils et al. 2005; Bean et al. 2006), in stark contrast to their high-mass counterparts. However, recent results have shown that the M dwarfs with attending planets appear to be metal-rich (see Section 2; Johnson & Apps 2009). With low-mass dwarfs becoming important sites for planet hunting (e.g. MEarth; Irwin et al. 2009; Endl et al. 2003; Johnson et al. 2007), the observational efficiency of these searches could be vastly increased with prior knowledge of stellar metallicity.

Because the ages of low-mass dwarfs span the lifetime of the Milky Way, they can provide important insight into the history and evolution of the Galaxy. Recent improvements in kinematic modeling and magnetic activity analysis have provided enhanced statistical age estimates for populations of low-mass dwarfs (West et al. 2006, 2008). Coupled with metallicity information, these ages can provide valuable insight into the chemical evolution history of the Milky Way disks. Without large samples of low-mass dwarfs, the utility of the statistically derived ages is limited. Fortunately, the advent of large surveys such as SDSS and 2MASS has produced photometric samples of low-mass dwarfs that number in the tens of millions (Bochanski et al. 2010) and spectroscopic samples that contain more than 70,000 M dwarfs (West et al. 2008; Kruse et al. 2010; West et al. 2010) and almost 500 L dwarfs (Schmidt et al. 2010b). In addition, these large catalogs of low-mass dwarfs have identified significant samples of metal-poor subdwarfs. The detailed metallicities of these objects, coupled with their kinematic distributions, establish important constraints on the structure and composition of the Milky Way halo.

Historically, the metallicity of low-mass dwarfs has been an elusive fundamental property due to the complex atmospheres of M, L and T dwarfs that have restricted the accuracy of detailed model atmospheres. Over the past several years, new observational techniques as well as independent theoretical advancements in atmospheric models have produced results that appear to link the metallicity of low-mass dwarfs to both their photometric and spectroscopic properties (e.g., Bean et al. 2006; Bonfils et al. 2005; Woolf & Wallerstein 2006; Johnson & Apps 2009; Hauschildt & Baron 2010; Rojas-Ayala et al. 2010). While these relations and the resulting metallicities provide fundamental measurements for stellar astrophysics, they also play a crucial role in studies of Galactic evolution and the environments that host extrasolar planets.

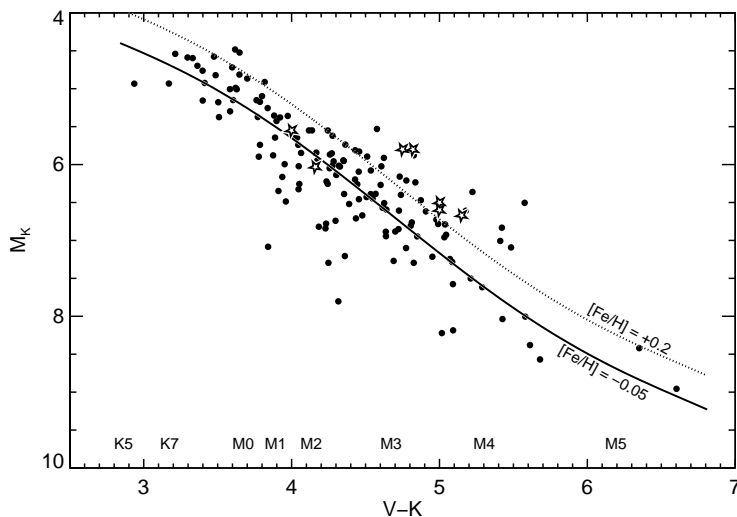


Figure 1. The low-mass target stars of the California Planet Survey in the M_K vs $V - K$ plane (filled circles), and the M dwarfs known to harbor one or more gas giant planets (five-point stars). The isometallicity contours for $[\text{Fe}/\text{H}] = 0$ (solid) and $[\text{Fe}/\text{H}] = +0.2$ (dotted line) are based on the broad-band photometric metallicity calibration of Johnson & Apps (2009).

2. Calibrating M Dwarf Metallicity using Photometry

Several previous studies have estimated M dwarf metallicities using wide binary pairs that consist of both an M dwarf and a higher mass star (e.g., Bean et al. 2006; Bonfils et al. 2005; Woolf & Wallerstein 2006). Because binaries are assumed to be both coeval and have the same metallicity, the composition of the higher mass star (which can be accurately derived from comparison to theoretical models) can be applied to the companion M dwarf. Some of these studies have used optical and infrared spectroscopy to tie spectroscopic features to a metallicity scale (e.g., Bean et al. 2006; Woolf et al. 2009; Rojas-Ayala et al. 2010). Although the spectroscopic method has shown great promise in deriving M dwarf metallicities (see Section 3), spectroscopy is considerably more time consuming than photometry and may not be easy to obtain for large samples of stars.

Bonfils et al. (2005) used M dwarfs in wide binaries to derive a relation between the absolute K -band magnitude and the $V - K$ color (higher metallicity M dwarfs are slightly brighter at a given color). Given the large number of M dwarfs for which there exist photometric observations, this relation may prove exceedingly useful. However, there were 2 problems with resulting analyses: 1) using the Bonfils et al. (2005) relation, planet hosting M dwarfs appeared to be metal poor compared to their FGK star counterparts; and 2) the relation yielded a mean metallicity of M dwarfs in the solar neighborhood that was almost 0.1 dex below the mean $[\text{Fe}/\text{H}]$ of higher mass stars. These discrepancies were resolved by Johnson & Apps (2009), who discovered a systematic uncertainty in the photometry used by Bonfils et al. (2005). Johnson & Apps

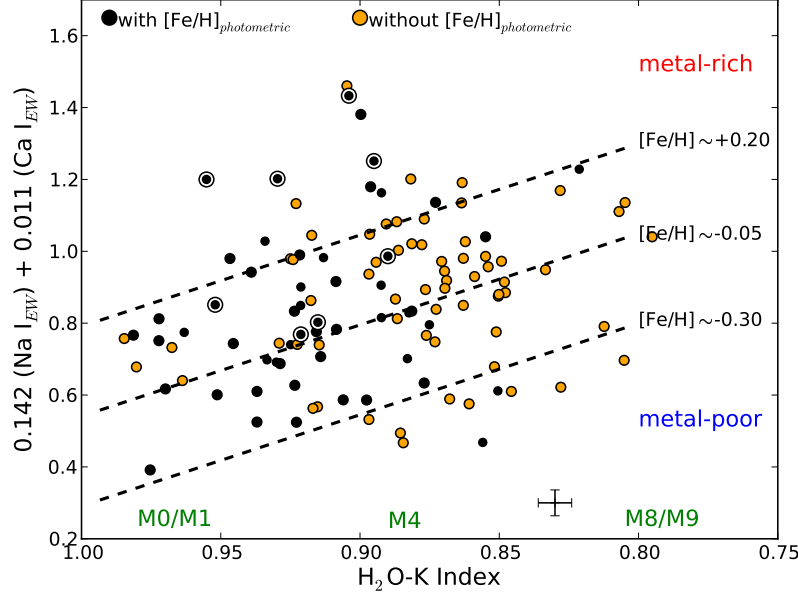


Figure 2. A linear combination of the EWs of the Ca I and Na I features versus the H_2O-K index for northern 8 pc M-dwarfs. The black dots represent M dwarfs with photometric metallicities and the yellow dots represent M dwarfs with only near-infrared (NIR) spectroscopic metallicities. The big black dots (with circles) represent the M dwarf planet hosts. Typical errors in EWs and H_2O-K index are represented by the error bars. The dashed lines in the top panel are iso-metallicity contours for $[Fe/H]$ values of -0.30, -0.05 and +0.20, calculated from the NIR $[Fe/H]$ calibration. The NIR $[Fe/H]$ calibration allows to cover a larger sample of cooler and distant M dwarfs (yellow dots)

(2009) used corrected photometry to re-derive a relation between the metallicity, M_K and $V - K$ color of M dwarfs (see also Schlaufman & Laughlin 2010).

Figure 1 shows the low-mass target stars of the California Planet Survey in the M_K vs $V - K$ plane (filled circles), and the M dwarfs known to harbor one or more gas giant planets (five-point stars). The isometallicity contours for $[Fe/H] = 0$ (solid) and $[Fe/H] = +0.2$ (dotted line) are based on the broad-band photometric metallicity calibration of Johnson & Apps (2009). The distribution of stars illustrates the tendency of planet-hosting M dwarfs to be metal-rich compared to stars in the Solar Neighborhood. The planet-metallicity relationship therefore holds for M dwarfs as well as Sun-like FGK stars.

3. Calibrating M Dwarf Metallicity using Infrared Spectroscopy

Most of the attempts to estimate the overall metal content of M dwarfs have been performed at visible wavelengths (e.g., Gizis 1997; Bonfils et al. 2005; Johnson & Apps 2009). Since M dwarfs are optically faint, this limited past analyses to early-type M dwarfs and few specific nearby stars, which are bright and have accurate parallaxes. To avoid this limitation, Rojas-Ayala et al. (2010) developed a near-infrared

(NIR) [Fe/H] spectroscopic calibration using strong absorption features in the *K*-band spectra of M dwarfs. Rojas-Ayala et al. (2010) adopted a similar approach to that of Bonfils et al. (2005) and Johnson & Apps (2009), assuming that binary systems share the same metallicity since both components formed from the same original molecular cloud. Seventeen FGK+M binary systems in the SPOCS catalog (Valenti & Fischer 2005) were used as metallicity calibrators. The NIR [Fe/H] calibration uses the Equivalent Widths (EWs) of the Na I doublet and the Ca I triplet, and a water absorption index (H₂O, Covey et al. 2010) to differentiate between metal-rich and metal-poor M dwarfs ($\sigma \sim 0.15$ dex). The results obtained with the NIR spectroscopic [Fe/H] calibration are in agreement with the results obtained with the photometric calibration by Johnson & Apps (2009). The eight M dwarf planet hosts analyzed by Rojas-Ayala et al. (2010) have metallicities higher than -0.05 dex, with the Jovian planets hosts being more metal-rich than their Neptune analogs. This corroborates the Johnson & Apps (2009) conclusion that planets are found preferentially around metal-rich stars, like in their Sun-like counterparts.

As a moderate resolution *K*-band spectrum can be efficiently obtained for most M dwarfs with current spectrographs (e.g. TripleSpec, FIRE), the NIR [Fe/H] calibration allows observations of cooler and distant M dwarfs (Figure 2). Thus, this technique will enable the identification of likely planet hosts at lower masses than is possible with optical [Fe/H] techniques. However, the NIR [Fe/H] calibration is currently limited to M dwarf spectral types earlier than $\sim M7$ and $[Fe/H] > -0.7$, due to the lack of FGK dwarf/late-type M dwarf wide binary systems with measured spectroscopic metallicities, and subdwarfs with $\lambda/\Delta\lambda \approx 3000$ NIR spectra, to be used as calibrators.

4. Spectral Features of Low-Metallicity Brown Dwarfs

Brown dwarfs are expected to have a similar metallicity distribution to the stellar components of our Galaxy, but reliably determining the chemical compositions of individual brown dwarfs is a difficult task. Atmospheric models remain largely untested at non-solar metallicities, and there are no known benchmark brown dwarf companions to stars with significantly super- or sub-solar chemical compositions ($[Fe/H] \gtrsim +0.3$ or $[Fe/H] \lesssim -0.3$). The latest-type ultracool subdwarf companion known is the d/sdM9 benchmark HD 114762B ($[Fe/H] = -0.7$); atmospheric models do a reasonably good job of reproducing the medium-resolution ($\lambda/\Delta\lambda \sim 3800$) near-infrared spectral features of this object, but fits to the low resolution ($\lambda/\Delta\lambda \sim 150$) near-infrared spectrum are unreliable (Bowler et al. 2009).

Although atmospheric models are not yet grounded by brown dwarfs with known metallicities, trends in the models have provided qualitative indications of deviations from solar metallicity for a growing number of L and T dwarfs with peculiar spectra. The optical spectra of peculiar L dwarfs are marked most notably by enhanced metal-hydride and metal-oxide bands compared to normal L dwarfs of the same spectral type (Figure 3). These variations are likely caused by subsolar metallicities and possibly suppressed condensate formation. A reduced metallicity also increases collision-induced absorption by H₂ (CIA H₂), resulting in bluer NIR colors for a given optical spectral type. Cloud properties also influence the NIR colors of L dwarfs and there is no clear way to distinguish clouds from a mild deviation from solar metallicity from NIR colors or spectra alone (Burgasser et al. 2008). Among the ~ 20 known objects that make up this class of “blue L dwarfs” (Kirkpatrick et al. 2010), which is distinct from L subd-

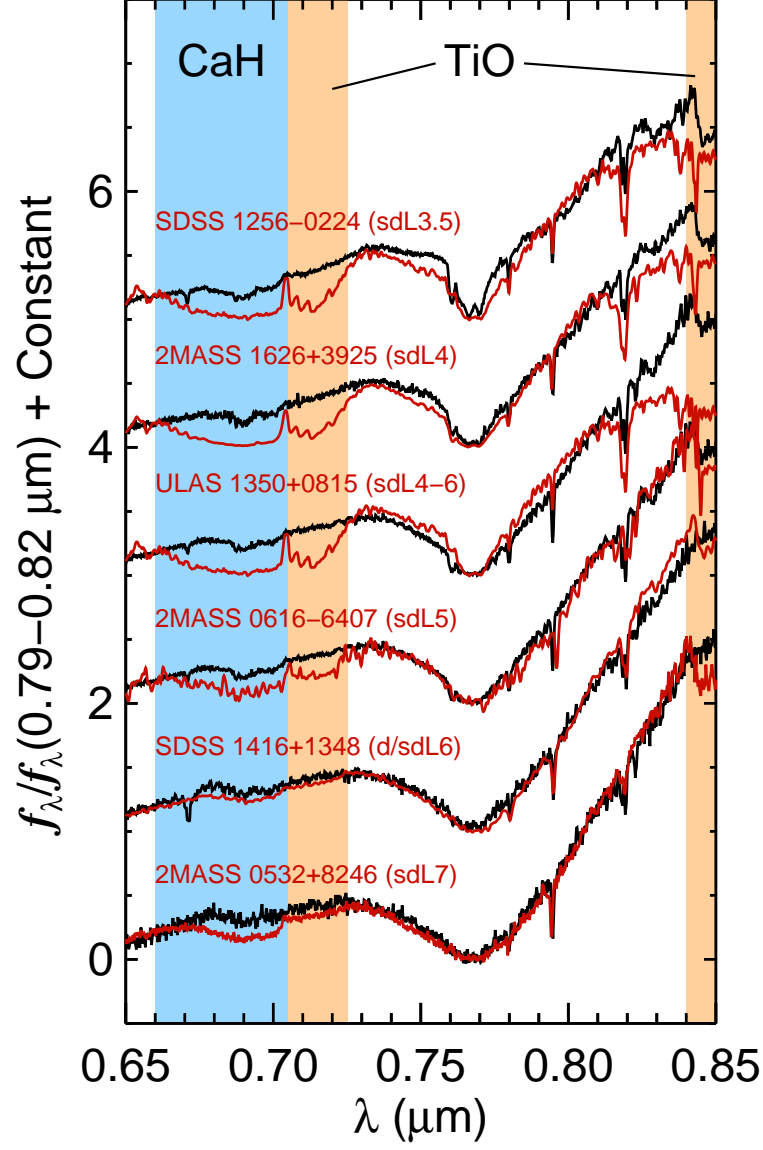


Figure 3. Optical spectra of L subdwarfs (red). The most notable differences in metal-poor L dwarfs compared to ordinary field objects are a stronger CaH absorption band at 6800 Å and stronger TiO absorption bands at 7100 Å and 8400 Å. From top to bottom the optical spectra originate from Burgasser et al. (2009), Burgasser et al. (2007), Lodieu et al. (2010), Cushing et al. (2009), Bowler et al. (2010), and Burgasser et al. (2003). Comparison spectra (black) are from Kirkpatrick et al. (1999); from top to bottom they are 2MASS 1146+2230 (L3), 2MASS 1155+2307 (L4), DENIS-P J1228.2–1547 (L5), DENIS-P J1228.2–1547 (L5), 2MASS 0850+1057 (L6), and DENIS-P J0205.4–1159 (L7). The spectra are normalized between 7900 Å and 8200 Å and are offset by a constant.

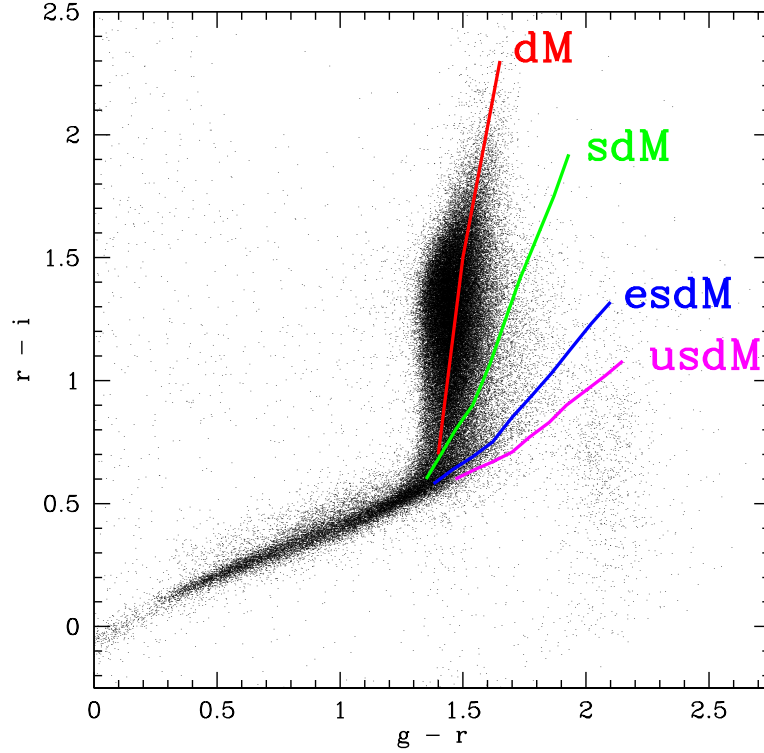


Figure 4. The $r-i$ vs. $g-r$ color-color diagram for stars in the SDSS spectroscopic catalog. The thick colored lines show the mean loci for the 4 metallicity classes of M dwarfs (dM:red; sdM:green; esdM:blue; and usdM :purple).

warfs, two benchmark blue L dwarfs provide important clues about the nature of the spectral peculiarities. The blue L dwarf 2MASS J17114559+4028578 (L4.5) orbits a solar-metallicity star (Radigan et al. 2008) and the blue L dwarf SDSS J141624.08+134826.7 (d/sdL6, Bowler et al. 2010; Schmidt et al. 2010a) has a peculiar T7.5 companion with spectral features indicative of being mildly metal-poor (Burningham et al. 2010; Burgasser et al. 2010); this is the first evidence that blue L dwarfs may span a range of metallicities. For T dwarfs, gravity and metallicity both affect the K -band flux by influencing CIA H_2 (e.g., Liu et al. 2007). Metallicity (and to a lesser extent gravity) also affects the Y -band flux, offering a way to distinguish between these parameters (e.g., Leggett et al. 2007). Ongoing sensitive all-sky surveys like WISE and Pan-STARRS are expected to greatly increase the census of non-solar metallicity isolated and benchmark L and T dwarfs, enabling rigorous testing of atmospheric models and an empirical calibration of spectral classification schemes.

5. The Colors and sub-Classes of Subdwarfs in SDSS

Low-mass stars with very low metallicities, typical of the Galactic thick disk and halo population, have a spectral energy distribution that is significantly different from the

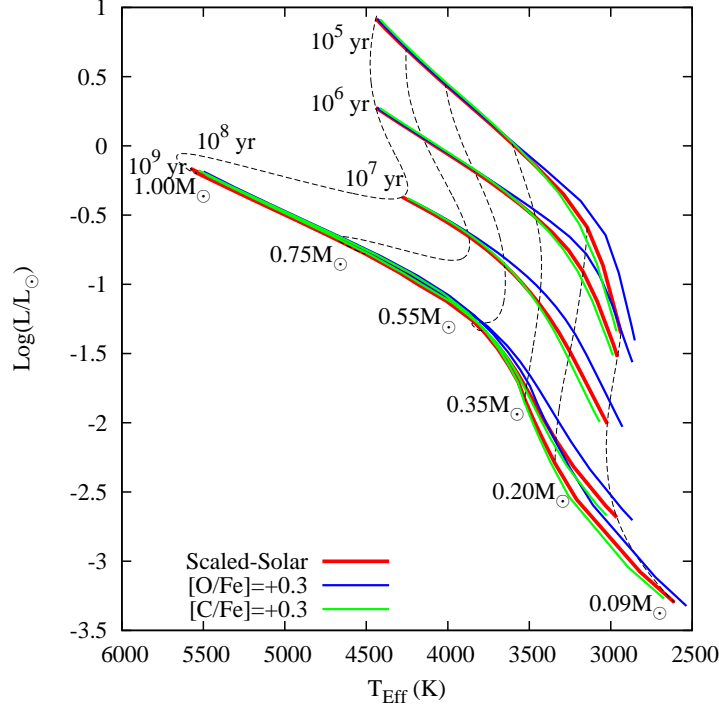


Figure 5. Luminosity vs. temperature diagram for a series of isochrones with masses between 0.09 and $1 M_{\odot}$ and ages between 10^5 and 10^9 years with $[\text{Fe}/\text{H}]=0$. The red lines have Solar C and O abundances, while the blue and green lines are enhanced in O and C respectively.

more metal-rich disk stars. The reason lies in the reduced absorption from metal oxide bands, in particular TiO. M dwarfs are classified in four so-called “metallicity classes” based on the relative strengths of their TiO bands: from the metal-rich dwarf M dwarfs (dM), to subdwarfs (sdM), extreme subdwarfs (esdM), and the very metal-poor ultra-subdwarfs (usdM). The classification follows the system of Gizis (1997) recently upgraded by Lépine et al. (2007). The sequence $\text{usdM} \rightarrow \text{esdM} \rightarrow \text{sdM} \rightarrow \text{dM}$ is believed to form a sequence of increasing metallicity (Gizis & Reid 1997; Woolf et al. 2009), with $[\text{Fe}/\text{H}] \approx -0.5$ for sdM, $[\text{Fe}/\text{H}] \approx -1.0$ for esdM, and $[\text{Fe}/\text{H}] \lesssim -1.5$ for usdM, although the metallicity calibration remain relatively uncertain to this date.

A recent search of the Sloan Digital Sky Survey (SDSS) spectroscopic database (Lépine et al. in preparation) has produced over 7,600 M subdwarfs. Their color distribution reveals significant differences with the metallicity class. Figure 4 shows the $r - i$ color as a function of $g - r$. The dots show a typical distribution for nearby field stars, displaying the well-known “elbow” with a strong inflection point at $g - r = 1.4$, $r - i = 0.6$. The thick colored lines show the mean loci for the dM (red), sdM (green), esdM (blue), and usdM (purple). There is a clear segregation as a function of the metallicity class, which reflects the strong effect that the TiO bands have on the spectral energy distribution. Ultrasubdwarfs simply extend the linear relationship between $g - r$ and $r - i$, as one would expect from a blackbody. As the metallicity increases, the “elbow” becomes increasingly pronounced. This happens because the r -band gets increasingly depressed in the more metal rich stars, as the TiO opacity increases. This

strong dependence of color on metallicity opens the possibility of estimating metallicities in low-mass stars based on broadband photometry alone. As it turns out, even dM show a significant scatter in $g - r$ which could be entirely explained by differences in metallicity. Should this be confirmed, this would provide a formidable tool for quick and easy metallicity estimates of low-mass stars. A proper calibration of the $g - r$ and $r - i$ color terms as a function of metallicity should be a priority.

6. Metallicity and Stellar Evolution Models

“Metallicity” loosely describes the heavy element content of a star or stellar population. Metallicity and $[\text{Fe}/\text{H}]$ are often used interchangeably, with the implicit assumption that the other heavy elements scale with Fe as they do in the Sun. If they don’t, then it’s important to understand how changing a given element alters the spectrum, hence the opacity, hence the effective temperature scale of the star (Dotter et al. 2007).

After H and He, the two most abundant elements in the sun by mass or number fraction are C and O (e.g., Asplund et al. 2009). When C or O is enhanced relative to solar at fixed $[\text{Fe}/\text{H}]$ the most dramatic effect appears in the molecular opacities. Figure 5 shows a series of isochrones with masses between 0.09 and 1 M_{\odot} and ages between 10^5 and 10^9 years with $[\text{Fe}/\text{H}]=0$. As Figure 5 indicates, on the one hand, enhancing C actually makes the lowest mass stars hotter while, on the other hand, enhancing O makes them cooler. This behavior can be understood in terms of the contribution of water molecules to the opacity. When analyzing the physical properties of low mass stars with effective temperatures below about 4,000K it is important to consider that non-solar abundance ratios can skew the results.

7. Metallicity and Atmosphere Models

One of the primary tools for measuring metallicities of low-mass objects is the comparison of data to synthetic spectra (created using atmospheric models). Calculating such models is common practice (e.g., Sordo et al. 2010) using modern atmosphere codes (Hauschildt & Baron 1999). For low-mass objects in general, it is crucial to account for dust formation in the atmosphere. This dust formation needs to be treated as a microphysical growth and destruction process (e.g. Helling et al. 2008). Furthermore, molecules, both as an opacity source and as material that affects the equation of state, need to be accounted for with accurate input data such as formation constants or related quantities and line lists or equivalent opacity data. The situation is further complicated when calculating models specifically for low metallicity objects, such as the models of Witte et al. (2009). The decreasing metal content does not change or even simplify any of the main physical processes, but, in contrast, adds another dimension of parameter space. In particular, dust keeps forming in significant amounts down to metallicities of about $[\text{Fe}/\text{H}]=-4.0$ (Witte et al. 2009).

Recently, it has become possible to apply synthetic spectra to observations of L subdwarfs and to attempt to measure metallicities (Burgasser et al. 2009). However, the quality of the fits and the derived metallicities still vary (Witte et al. 2010) depending on the quality of the implemented physics (see also Fig. 6). However, it is worth noting that the derived metallicities of the sdL class do not need to be the same of the sdM class as derived by e.g. Gizis (1997) or Schweitzer (1999). Measuring metallicities directly

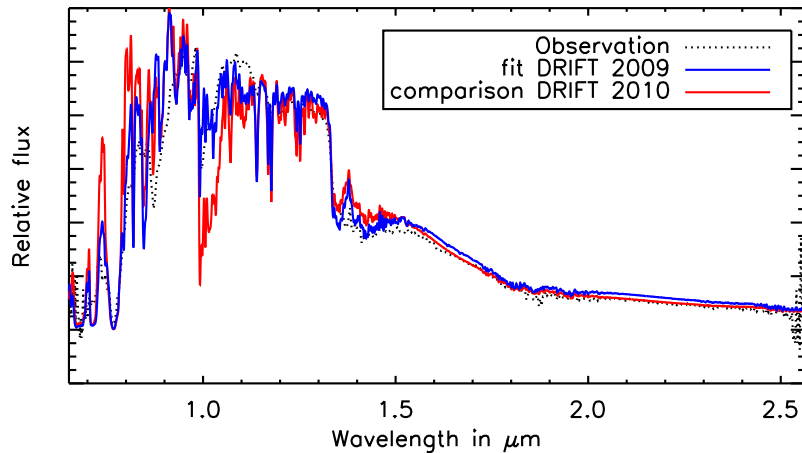


Figure 6. The sdL4 dwarf 2MASS1626+3925 (black, dotted; Burgasser 2004) and a fit with the DRIFT 2009 models (blue, solid; Witte et al. 2009). The comparison with the DRIFT 2010 models (red, solid; Witte et al. 2010) is a comparison with the same model parameters showing the differences in model details. Both models have $T_{\text{eff}} = 2100\text{K}$, $\log(g)=5.0$ and a metallicity $[\text{Fe}/\text{H}] = -1.5$.

at a resolution of 0.1 dex or higher has not been attempted yet since the molecular background lines add too much uncertainty.

8. Conclusions

During the first half of the last century, spectroscopic observations and radiative transfer theory began to unlock the composition of stars. Determining the metallicity of stars has been very important to a wide range of astronomical investigations, from planetary to cosmological scales. Yet, despite the progress made for most of the main sequence, measuring the metallicity of the Galaxy's most populous members, M dwarfs, remains a daunting task.

At the start of this century, astronomers are beginning to unlock the metal content of these stars. However, there is much work to be done by both observers and theorists. Observationally, there are promising new results suggesting that IR observations may be important for estimating metallicities. This is strengthened by the relative agreement between models and spectra in this regime. However, these methods need further testing (with M dwarf binaries or clusters). In the optical bandpass, the relative metallicity classes described in Section 5 display a clear separation in photometric colors. This will be crucial for estimating the metal content of these stars in the next generation of surveys, which will be largely photometric. Yet, these classes have not been rigorously tied to an absolute metallicity scale. Once this occurs, the chemical composition of M dwarfs will be a powerful tool for studying the Galaxy and identifying the most likely exoplanet hosts. Identifying new benchmarks, for both M dwarfs and brown dwarfs, will be crucial in calibrating optical observations.

On the theoretical front, new line lists, opacity calculations and the inclusion of dust grains have resulted in better agreement with observations. The effects of carbon and oxygen abundance differences can be modeled and explain observations of the lower main sequence of globular clusters. As computational power and techniques advance, these models will grow in sophistication and should offer a more realistic picture of the important physics within these stars.

Unlocking the metallicity of M dwarfs will profoundly benefit the astronomical community in a variety of ways, such as identifying exoplanet hosts and studying chemical evolution. The work presented here represents the first steps in solving this problem.

Acknowledgments. The authors would like to thank the Cool Stars 16 SOC for the opportunity to hold this productive splinter session. BPB gratefully acknowledges the Cool Stars 16 Accommodation Stipend Award, funded by the NASA Astrobiology Institute.

References

- Asplund, M., Grevesse, N., Sauval, A. J., & Scott, P. 2009, *ARA&A*, 47, 481. 0909.0948
- Bean, J. L., Benedict, G. F., & Endl, M. 2006, *ApJ*, 653, L65. arXiv:astro-ph/0611060
- Bochanski, J. J., Hawley, S. L., Covey, K. R., West, A. A., Reid, I. N., Golimowski, D. A., & Ivezić, Ž. 2010, *AJ*, 139, 2679. 1004.4002
- Bonfils, X., Delfosse, X., Udry, S., Santos, N. C., Forveille, T., & Ségransan, D. 2005, *A&A*, 442, 635. arXiv:astro-ph/0503260
- Bowler, B. P., Liu, M. C., & Cushing, M. C. 2009, *ApJ*, 706, 1114. 0910.1604
- Bowler, B. P., Liu, M. C., & Dupuy, T. J. 2010, *ApJ*, 710, 45. 0912.3796
- Burgasser, A. J. 2004, *ApJ*, 614, L73. arXiv:astro-ph/0409179
- Burgasser, A. J., Cruz, K. L., Cushing, M., Gelino, C. R., Looper, D. L., Faherty, J. K., Kirkpatrick, J. D., & Reid, I. N. 2010, *ApJ*, 710, 1142. 0912.3808
- Burgasser, A. J., Cruz, K. L., & Kirkpatrick, J. D. 2007, *ApJ*, 657, 494. arXiv:astro-ph/0610096
- Burgasser, A. J., Kirkpatrick, J. D., Burrows, A., Liebert, J., Reid, I. N., Gizis, J. E., McGovern, M. R., Prato, L., & McLean, I. S. 2003, *ApJ*, 592, 1186. arXiv:astro-ph/0304174
- Burgasser, A. J., Looper, D. L., Kirkpatrick, J. D., Cruz, K. L., & Swift, B. J. 2008, *ApJ*, 674, 451. 0710.1123
- Burgasser, A. J., Witte, S., Helling, C., Sanderson, R. E., Bochanski, J. J., & Hauschildt, P. H. 2009, *ApJ*, 697, 148. 0903.1567
- Burningham, B., Leggett, S. K., Lucas, P. W., Pinfield, D. J., Smart, R. L., Day-Jones, A. C., Jones, H. R. A., Murray, D., Nickson, E., Tamura, M., Zhang, Z., Lodieu, N., Tinney, C. G., & Zapatero Osorio, M. R. 2010, *MNRAS*, 404, 1952. 1001.4393
- Covey, K. R., Lada, C. J., Román-Zúñiga, C., Muench, A. A., Forbrich, J., & Ascenso, J. 2010, *ApJ*, 722, 971. 1007.2192
- Cushing, M. C., Looper, D., Burgasser, A. J., Kirkpatrick, J. D., Faherty, J., Cruz, K. L., Sweet, A., & Sanderson, R. E. 2009, *ApJ*, 696, 986. 0902.1059
- Dotter, A., Chaboyer, B., Ferguson, J. W., Lee, H., Worthey, G., Jevremović, D., & Baron, E. 2007, *ApJ*, 666, 403. 0706.0808
- Endl, M., Cochran, W. D., Tull, R. G., & MacQueen, P. J. 2003, *AJ*, 126, 3099. arXiv:astro-ph/0308477
- Fischer, D. A., & Valenti, J. 2005, *ApJ*, 622, 1102
- Gizis, J., & Reid, I. 1997, *PASP*, 109, 1233. arXiv:astro-ph/9708244
- Gizis, J. E. 1997, *AJ*, 113, 806. arXiv:astro-ph/9611222
- Hauschildt, P. H., & Baron, E. 1999, *Journal of Computational and Applied Mathematics*, 109, 41. arXiv:astro-ph/9808182

- 2010, *A&A*, 509, A36+. 0911.3285
- Helling, C., Woitke, P., & Thi, W. 2008, *A&A*, 485, 547. 0803.4315
- Irwin, J., Charbonneau, D., Berta, Z. K., Quinn, S. N., Latham, D. W., Torres, G., Blake, C. H., Burke, C. J., Esquerdo, G. A., Fürész, G., Mink, D. J., Nutzman, P., Szentgyorgyi, A. H., Calkins, M. L., Falco, E. E., Bloom, J. S., & Starr, D. L. 2009, *ApJ*, 701, 1436. 0906.4365
- Johnson, J. A., & Apps, K. 2009, *ApJ*, 699, 933. 0904.3092
- Johnson, J. A., Butler, R. P., Marcy, G. W., Fischer, D. A., Vogt, S. S., Wright, J. T., & Peek, K. M. G. 2007, *ApJ*, 670, 833. 0707.2409
- Kirkpatrick, J. D., Looper, D. L., Burgasser, A. J., Schurr, S. D., Cutri, R. M., Cushing, M. C., Cruz, K. L., Sweet, A. C., Knapp, G. R., Barman, T. S., Bochanski, J. J., Roellig, T. L., McLean, I. S., McGovern, M. R., & Rice, E. L. 2010, *ApJS*, 190, 100. 1008.3591
- Kirkpatrick, J. D., Reid, I. N., Liebert, J., Cutri, R. M., Nelson, B., Beichman, C. A., Dahn, C. C., Monet, D. G., Gizis, J. E., & Skrutskie, M. F. 1999, *ApJ*, 519, 802
- Kruse, E. A., Berger, E., Knapp, G. R., Laskar, T., Gunn, J. E., Loomis, C. P., Lupton, R. H., & Schlegel, D. J. 2010, *ApJ*, 722, 1352. 0911.2712
- Leggett, S. K., Marley, M. S., Freedman, R., Saumon, D., Liu, M. C., Geballe, T. R., Golimowski, D. A., & Stephens, D. C. 2007, *ApJ*, 667, 537. 0705.2602
- Lépine, S., Rich, R. M., & Shara, M. M. 2007, *ApJ*, 669, 1235. 0707.2993
- Liu, M. C., Leggett, S. K., & Chiu, K. 2007, *ApJ*, 660, 1507. [arXiv:astro-ph/0701111](#)
- Lodieu, N., Zapatero Osorio, M. R., Martín, E. L., Solano, E., & Aberasturi, M. 2010, *ApJ*, 708, L107. 0912.3364
- Radigan, J., Lafrenière, D., Jayawardhana, R., & Doyon, R. 2008, *ApJ*, 689, 471. 0808.1575
- Rojas-Ayala, B., Covey, K. R., Muirhead, P. S., & Lloyd, J. P. 2010, *ApJ*, 720, L113
- Schlaufman, K. C., & Laughlin, G. 2010, *A&A*, 519, A105+. 1006.2850
- Schmidt, S. J., West, A. A., Burgasser, A. J., Bochanski, J. J., & Hawley, S. L. 2010a, *AJ*, 139, 1045. 0912.3565
- Schmidt, S. J., West, A. A., Hawley, S. L., & Pineda, J. S. 2010b, *AJ*, 139, 1808. 1001.3402
- Schweitzer, A. 1999, Ph.D. thesis, PhD Thesis, Landessternwarte Heidelberg/Königstuhl (1999).
- Sordo, R., Vallenari, A., Tantaló, R., Allard, F., Blomme, R., Bouret, J., Brott, I., Fremat, Y., Martayan, C., Damerdjí, Y., Edvardsson, B., Josselin, E., Plez, B., Kochukhov, O., Kontizas, M., Munari, U., Saguner, T., Zorec, J., Schweitzer, A., & Tsalmantza, P. 2010, *Ap&SS*, 328, 331
- Valenti, J. A., & Fischer, D. A. 2005, *ApJS*, 159, 141
- West, A. A., Bochanski, J. J., Hawley, S. L., Cruz, K. L., Covey, K. R., Silvestri, N. M., Reid, I. N., & Liebert, J. 2006, *AJ*, 132, 2507. [arXiv:astro-ph/0609001](#)
- West, A. A., Hawley, S. L., Bochanski, J. J., Covey, K. R., Reid, I. N., Dhital, S., Hilton, E. J., & Masuda, M. 2008, *AJ*, 135, 785. 0712.1590
- West, A. A., et al. 2010, *AJ*, submitted
- Witte, S., Helling, C., & Hauschildt, P. H. 2009, *A&A*, 506, 1367. 0908.3597
- Witte, S., et al. 2010, *A&A*, submitted
- Woolf, V. M., Lépine, S., & Wallerstein, G. 2009, *PASP*, 121, 117
- Woolf, V. M., & Wallerstein, G. 2006, *PASP*, 118, 218. [arXiv:astro-ph/0510148](#)